Encounter-Limited Charge-Carrier Recombination in Phase-Separated Organic Semiconductor Blends

Michael C. Heiber,[1,2,*] Christoph Baumbach,[2] Vladimir Dyakonov,[1,3] and Carsten Deibel[2,†]
[1]Experimental Physics VI, Julius-Maximilians-University of Würzburg, 97074 Würzburg, Germany
[2]Institut für Physik, Technische Universität Chemnitz, 09126 Chemnitz, Germany
[3]Bavarian Centre for Applied Energy Research (ZAE Bayern), 97074 Würzburg, Germany
(Received 11 September 2014; revised manuscript received 23 January 2015; published 1 April 2015)

The theoretical effects of phase separation on encounter-limited charge carrier recombination in organic semiconductor blends are investigated using kinetic Monte Carlo simulations of pump-probe experiments. Using model bulk heterojunction morphologies, the dependence of the recombination rate on domain size and charge carrier mobility are quantified. Unifying competing models and simulation results, we show that the mobility dependence of the recombination rate can be described using the power mean of the electron and hole mobilities with a domain-size-dependent exponent. Additionally, for domain sizes typical of organic photovoltaic devices, we find that phase separation reduces the recombination rate by less than one order of magnitude compared to the Langevin model and that the mobility dependence can be approximated by the geometric mean.

DOI: 10.1103/PhysRevLett.114.136602 PACS numbers: 72.20.Jv, 72.20.Ee, 81.05.Fb, 88.40.jr

Despite vast scientific investigations on organic electronic devices over the last two decades, significant gaps in fundamental understanding exist in key areas. A detailed description of charge carrier recombination, important for designing organic photovoltaics (OPVs), organic light-emitting diodes, and organic photodiodes, is a work in progress. To continue improving these devices, the dominant factors controlling recombination processes must be understood further so that they can be carefully controlled in energy efficient devices.

Bimolecular charge recombination in organic semiconductors is most commonly described as a second-order reaction following the Langevin model [1],

$$R = k_L np, \tag{1}$$

where k_L is the Langevin recombination coefficient and n and p are the concentrations of electrons and holes, respectively. k_L is derived by assuming an encounter-limited reaction in which the time it takes for an electron and hole to come together due to their Coulomb attraction is rate limiting. As a result,

$$k_L = \frac{e}{\epsilon\epsilon_0}(\mu_e + \mu_h), \tag{2}$$

where e is the elementary charge, ϵ is the dielectric constant, ϵ_0 is the vacuum permittivity, and μ_e and μ_h are the electron and hole mobilities, respectively.

The Langevin model also assumes a spatially and energetically homogeneous and isotropic system with no internal electric field, which is not strictly valid in most organic semiconducting devices. Organic semiconductors are well characterized as having varying degrees of energetic and spatial disorder that can have a major impact on charge transport properties as highlighted by the commonly used Gaussian disorder model (GDM) [2]. In addition, devices may operate with a significant internal electric field. Investigating these issues, a number of kinetic Monte Carlo (KMC) simulation studies have identified conditions where deviations from the Langevin model occur [3–7]. However, van der Holst *et al.* concluded that the Langevin model still works well in an isotropic system with the GDM at low electric fields as long as accurate mobility values are used [8]. In agreement, measurements on a number of neat organic semiconducting materials have been consistent with the Langevin model [9–12].

While the Langevin model may work well for neat materials, many devices utilize phase-separated blends [13]. In such blends, electrons and holes are relegated to separate phases and are only able to undergo recombination at the phase boundaries. The resulting spatial limitations on charge carrier motion and recombination locations are expected to alter the recombination kinetics. Bulk heterojunction (BHJ) OPVs with domain sizes ranging from approximately 10 to 50 nm have often exhibited two major deviations from the Langevin model. First, super-second-order recombination kinetics has been measured in several blend systems [14–20]. Often attributed to charge traps, the reasons for this behavior are still under debate [12,19,21–26].

The second major deviation, commonly observed in composite P3HT and PCBM films, is a recombination rate that is several orders of magnitude less than predicted by the Langevin model [16,27–29]. [P3HT denotes poly(3-hexylthiophene-2,5-diyl) and PCBM denotes phenyl–C61–butyric acid methyl.] As a result, Pivrikas *et al.* proposed that a reduced recombination rate is an inherent property of BHJ blends [27], and Koster *et al.* created the minimum mobility model, arguing that the recombination rate in a phase-separated system should be limited by the mobility of the slowest carrier [30],

$$k_{\min} = \frac{e}{\epsilon\epsilon_0}\min(\mu_e, \mu_h). \quad (3)$$

However, even though a significant reduction was also found in several other blends [31–36], some blend systems exhibit recombination rates much closer to the Langevin model [31,32,37–39]. It is becoming increasingly clear that a greatly reduced recombination rate is not an inherent property of phase-separated blends but is a property that is dependent on a number of factors that are still under debate [12,23,33,40–44].

Despite clear deviations in many cases, the Langevin model is often used to explain bimolecular recombination in phase-separated blends because a more complete model is still missing. An important first step towards a more complete model is understanding the fundamental effect of phase separation on encounter-limited bimolecular recombination. Previously, Groves and Greenham used KMC simulations to show that the recombination rate in a simple phase-separated system lies somewhere between the Langevin model and the minimum mobility model with a weak dependence on domain size [7]. In addition, some experiments have also indicated a relatively weak domain size dependence [34]. However, other KMC simulations [45] and experiments [36] have indicated that the domain size could have a larger impact.

In this Letter, we determine the dependence of the recombination rate on the domain size and the electron and hole mobilities. We find that with a very small domain size, the Langevin model still holds, but for larger domains, clear deviations are present. Unifying the competing Langevin and minimum mobility models with our simulation results, we show that the mobility dependence can be described using the power mean of the mobilities with a domain-size-dependent exponent. Additionally, for domain sizes typical of OPVs, we find that phase separation reduces the recombination rate by less than one order of magnitude compared to the Langevin model and that the mobility dependence can be approximated by the geometric mean.

Because of the complex geometry of phase-separated systems, analytical derivation of the recombination rate as a function of the domain size is extremely difficult. As a result, KMC simulations were performed to reach a numerical solution. The simulations were configured to simulate pump-probe experiments on BHJ films without electrodes. Using the ISING_OPV software tool, a simple Ising phase separation model was implemented to create morphologies with varying domain size from 5 to 55 nm [46,47]. For each domain size (d) tested, 100 morphologies were independently generated to form a morphology set. The resulting morphologies consist of two pure phases with equivalent average domain sizes in a bicontinuous network configuration.

The model morphologies were then implemented into a three-dimensional lattice with a lattice constant of 1 nm, and sites were assigned energies from an uncorrelated Gaussian DOS with an energetic disorder (σ) of 75 meV. Two-dimensional periodic boundary conditions were used to simulate a thin film. To start the simulation, excitons were created with uniform probability throughout the lattice with a Gaussian excitation pulse having a pulse width of 100 ps and an intensity corresponding to an initial exciton concentration of 5×10^{17} cm^{-3}. However, for 55 nm domains, the initial exciton concentration was set to 3.1×10^{17} cm^{-3} due to computational limitations. This change had no impact on the recombination behavior of interest in this study. The complexities of charge separation were bypassed to create free charge carriers directly from excitons. To do this, electron-hole pairs were created across the interface with a separation distance of 30 nm by restricting exciton creation to within 30 nm of an interface and executing an ultrafast long-range charge transfer event. The charges in the lattice then underwent hopping transport using the Miller-Abrahams (MA) model [48], and Coulomb interactions were included between charges within a cutoff radius of 35 nm. Electron hopping was restricted to acceptor domains and hole hopping was restricted to donor domains. Charge recombination was also implemented using the MA model with a recombination prefactor ($R_{0,\mathrm{rec}}$) that was held constant at a large value of 10^{15} s^{-1} to ensure that recombination dominated over redissociation.

For each simulation, 24 morphologies were randomly selected from the appropriate morphology set and 4 random configurations of energetic disorder were implemented for each, and the results of the 96 runs were averaged. During each simulation, the hole concentration was logged as a function of simulated time. With the lattice sizes used, the carrier concentration could be resolved over two and half orders of magnitude, covering a range typical for steady state illumination intensities from 0.1 to 10 suns. Assuming second-order recombination kinetics and $n = p$, the numerical derivative of the hole concentration as a function of time (t) was then used to calculate the simulated time-dependent recombination coefficient:

$$k_{\mathrm{sim}}(t) = -\frac{\frac{dp(t)}{dt}}{p(t)^2}. \quad (4)$$

In addition, the displacement of each carrier from its initial position was recorded over its lifetime, and the numerical derivative of the average mean squared displacement over time for all carriers was used to calculate the average time-dependent diffusion coefficient. Because of the thin film geometry, the two-dimensional diffusion equation was found to be most appropriate. Using the Einstein relation, which remains valid at zero field [4,49] when recombination removes deeply trapped carriers [50], the average time-dependent zero-field mobility of each carrier type was determined,

$$\mu(t) = \frac{e}{4k_B T}\frac{d\langle r(t)^2\rangle}{dt}. \quad (5)$$

More information about the morphology generation, KMC simulation parameters, and data analysis is shown in the Supplemental Material [51].

To determine the mobility dependence, the relative magnitudes of the electron and hole mobilities were tuned by varying the hole hopping prefactor ($R_{0,h}$) from 10^{11} to 10^{15} s^{-1} while holding the electron hopping prefactor ($R_{0,e}$) constant at 10^{13} s^{-1}. Figure 1 shows how the hole concentration (p) decays over time for differing magnitudes of $R_{0,h}$. By the time the hole concentration reached 10^{16} cm^{-3} (a typical concentration for 1 sun steady state illumination), all transients showed steady second-order decay. The time point where $p = 10^{16}$ cm^{-3} was used as the comparison point between different simulations. At this time point, the simulated recombination coefficient (k_{sim}), the mobilities (μ_e and μ_h), the Langevin recombination coefficient (k_L), and the minimum mobility model recombination coefficient (k_{min}) were calculated.

Figure 2 shows how the mobility dependence of the recombination coefficient changes with different magnitudes of domain size. With a very small domain size of 5 nm, the recombination rate approaches the Langevin model, and as the domain size increases, the recombination rate deviates from the Langevin model. In the intermediate regime, in agreement with the results of Groves and Greenham [7], the simulated recombination rate was neither found to be proportional to the sum of mobilities nor to the minimum mobility. Instead, a new trend not captured by any of the current models is observed, in which k_{sim} is approximately proportional to the geometric mean of the electron and hole mobilities. For the largest domain sizes tested, the mobility dependence continues to change as observed by the downward curvature beginning to form for $d = 45$ and 55 nm. Here, the mobility dependence appears to be approaching the shape predicted by the minimum mobility model. However, the bias toward the minimum mobility appears much weaker than predicted in the minimum mobility model. Another type of mean which favors the smaller value is the harmonic mean, and the simulated recombination behavior appears to be closer to the harmonic mean. The same general behavior was also observed when using different magnitudes of energetic disorder (σ) and when performing the analysis at carrier concentrations from 5×10^{15} to 2×10^{16} cm^{-3}.

To understand this behavior, consider a case where the electron has a very fast mobility compared to the hole. In a neat material, even if the hole is slow, it is still accessible to the electron everywhere. In this simple case, the resulting recombination rate is proportional to the sum of the individual mobilities as described in the Langevin model. Now, let us consider a phase-separated morphology with very small domains, as shown in Fig. 3(a). In this case, with highly interconnected domains and high interfacial area, the slow hole is still accessible to the electron almost everywhere. When the electron enters the Coulomb capture radius of the hole (depicted by the dashed circle), the attractive force becomes very strong and recombination occurs quickly. As a result, even though the electron and hole are restricted to separate phases, the resulting recombination rate should still follow the Langevin model.

However, with very large domains, as shown in Fig. 3(b), most of the slow holes are inaccessible to the electrons, and in order for recombination to occur, the hole must first

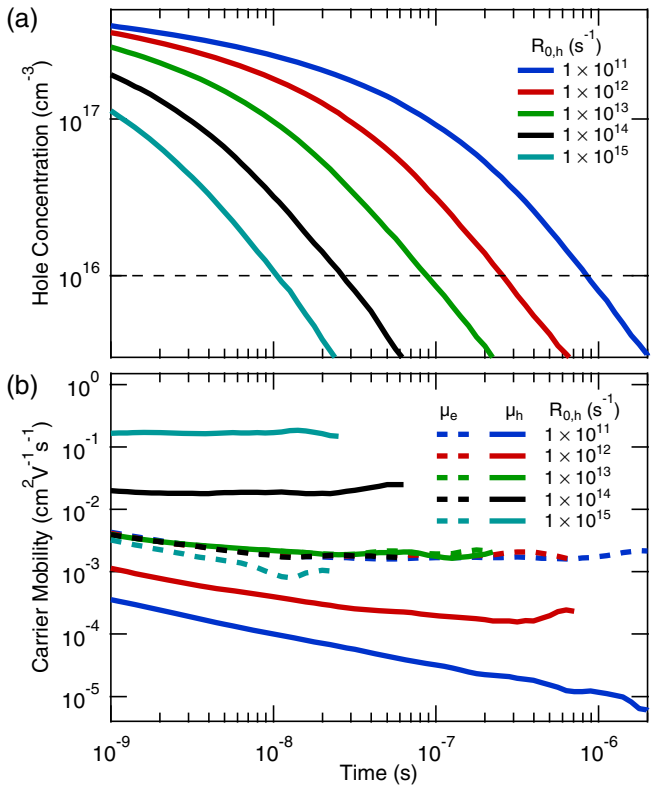

FIG. 1 (color online). (a) Hole concentration transients and (b) time-dependent mobilities for $d = 15$ nm with varying hole hopping rates.

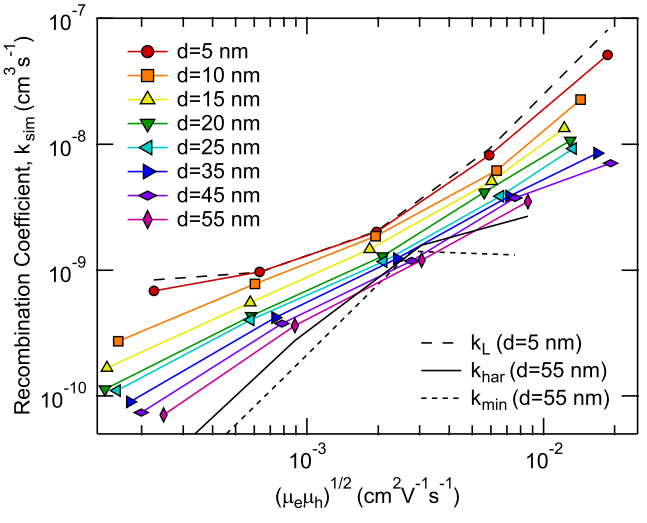

FIG. 2 (color online). The effect of the domain size on the mobility dependence of the simulated recombination rate coefficient compared to the Langevin, harmonic mean, and minimum mobility models.

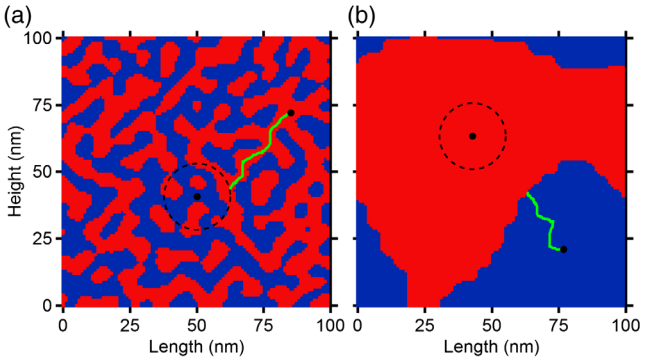

FIG. 3 (color online). Depiction of the two extreme recombination regimes: (a) very small domain size and (b) very large domain size. One charge is depicted with a dotted circle around it that represents the Coulomb capture radius (R_C). The other charge is shown with a green path that illustrates one of the most likely pathways to enter the capture sphere.

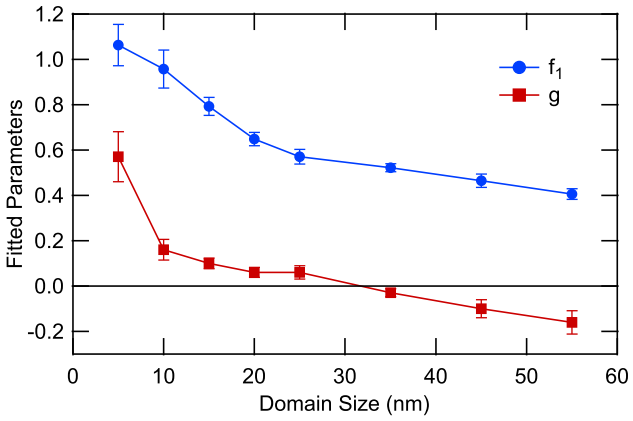

FIG. 4 (color online). Fitted values for the prefactor (f_1) and the power mean exponent (g) as a function of the domain size.

migrate to the interface. As a result, the recombination rate should be limited by the mobility of the slower hole and should follow the minimum mobility model. Given these two well-defined extreme cases, it follows logically that for intermediate domain sizes, the recombination behavior should be somewhere in between. In effect, the recombination rate of the slower carriers depends mainly on their distance from the interface. Those located right next to the interface will require almost no further motion, and their recombination rate will be dominated by the speed of the faster carrier. However, those located farther away will start to be limited more by their own slow motion, passing through a regime where the recombination rate will depend on the speed of both carriers and then eventually be dominated by the slow carrier when very far away. Given this behavior, when changing the domain size, the critical change is in the average distance between the carriers and the interface, which then alters the mobility dependence.

Capturing this behavior and unifying the competing analytical models with the simulations results of Groves and Greenham [7] and those presented here, all curves in Fig. 2 can be fit by the following simple equation (see Supplemental Material [51]),

$$k_{\mathrm{sim}} = \frac{e}{\epsilon\epsilon_0} f_1(d) 2 M_{g(d)}(\mu_e, \mu_h), \tag{6}$$

where $f_1(d)$ is a domain-size-dependent prefactor and $M_{g(d)}(\mu_e, \mu_h)$ is the power mean (generalized mean),

$$M_g(\mu_e, \mu_h) = \left(\frac{\mu_e^g + \mu_h^g}{2}\right)^{1/g}, \tag{7}$$

with a domain-size-dependent exponent $g(d)$. For a very small domain size, $\lim_{d\to 0} f_1(d) = 1$ and $\lim_{d\to 0} g(d) = 1$, and the Langevin expression is obtained. In addition, $\lim_{g\to 0} M_g$ is the geometric mean, M_{-1} is the harmonic mean, and $M_{-\infty}$ is the minimum value.

Figure 4 shows the fitted values for f_1 and g as a function of the domain size. For $d = 5$ nm, f_1 and g both approach one, meaning that the behavior is very close to the Langevin model. For intermediate domain sizes of about 10–35 nm, $g \approx 0$, meaning that the behavior in this regime can be approximated by the geometric mean. Then for $d > 35$ nm, g continues to slowly decrease, thereby increasing the impact of the minimum mobility.

In addition to the change in the mobility dependence, the magnitude of the recombination rate also decreases with increasing domain size. It is clear that simple phase separation alone causes only a mild reduction of less than one order of magnitude when the electron and hole mobilities are within one order of magnitude of each other, as is the case in most optimized devices. As a result, blends with much larger reductions must have other more dominant contributing factors. These blends are likely to be greatly affected by polaron pair redissociation and are therefore not in the encounter-limited regime and/or are affected by interfacial states different from those in the bulk [12].

In conclusion, we have quantified the effect of phase separation on the bimolecular charge recombination rate when in the encounter-limited regime. Most significantly, we have shown that the mobility dependence can be described by the power mean with a domain-size-dependent exponent. For domain sizes typical of OPVs, the geometric mean is a very good approximation of the mobility dependence. In addition, we clearly demonstrate that greatly reduced recombination rates are not an inherent property of phase-separated systems. These results represent a unification of previous recombination models and a major step forward in developing a more complete model for charge carrier recombination in organic semiconductor blends. With this knowledge, updated design rules for new materials and device architectures can be defined.

M. C. H. and C. D. acknowledge funding by Deutsche Forschungsgemeinschaft (DFG) Grant No. DE830/13-1. C. D. thanks Professor Michael Schreiber for a brief but helpful discussion. We also thank Dr. Kristofer Tvingstedt and Dr. Andreas Baumann for insightful discussion and feedback on the manuscript.

*heiber@mailaps.org
†deibel@physik.tu-chemnitz.de

[1] P. Langevin, Ann. Chim. Phys. **28**, 433 (1903).
[2] H. Bässler, Phys. Status Solidi B **175**, 15 (1993).
[3] B. Ries and H. Bässler, Chem. Phys. Lett. **108**, 71 (1984).
[4] R. Richert, L. Pautmeier, and H. Bässler, Phys. Rev. Lett. **63**, 547 (1989).
[5] U. Albrecht and H. Bässler, Chem. Phys. Lett. **235**, 389 (1995).
[6] Y. N. Gartstein, E. M. Conwell, and M. J. Rice, Chem. Phys. Lett. **249**, 451 (1996).
[7] C. Groves and N. C. Greenham, Phys. Rev. B **78**, 155205 (2008).
[8] J. J. M. van der Holst, F. W. A. van Oost, R. Coehoorn, and P. A. Bobbert, Phys. Rev. B **80**, 235202 (2009).
[9] P. W. M. Blom, M. J. M. de Jong, and S. Breedijk, Appl. Phys. Lett. **71**, 930 (1997).
[10] A. Pivrikas, G. Juška, R. Österbacka, M. Westerling, M. Viliūnas, K. Arlauskas, and H. Stubb, Phys. Rev. B **71**, 125205 (2005).
[11] S. L. M. van Mensfoort, J. Billen, M. Carvelli, S. I. E. Vulto, R. A. J. Janssen, and R. Coehoorn, J. Appl. Phys. **109**, 064502 (2011).
[12] J. Gorenflot, M. C. Heiber, A. Baumann, J. Lorrmann, M. Gunz, A. Kämpgen, V. Dyakonov, and C. Deibel, J. Appl. Phys. **115**, 144502 (2014).
[13] C. R. McNeill and N. C. Greenham, Adv. Mater. **21**, 3840 (2009).
[14] I. Montanari, A. F. Nogueira, J. Nelson, J. R. Durrant, C. Winder, M. A. Loi, N. S. Sariciftci, and C. Brabec, Appl. Phys. Lett. **81**, 3001 (2002).
[15] Y. Kim, S. Cook, S. M. Tuladhar, S. A. Choulis, J. Nelson, J. R. Durrant, D. D. C. Bradley, M. Giles, I. McCulloch, C.-S. Ha, and M. Ree, Nat. Mater. **5**, 197 (2006).
[16] C. Deibel, A. Baumann, and V. Dyakonov, Appl. Phys. Lett. **93**, 163303 (2008).
[17] G. Juška, K. Genevičius, N. Nekrašas, G. Sliaužys, and G. Dennler, Appl. Phys. Lett. **93**, 143303 (2008).
[18] T. M. Clarke, J. Peet, P. Denk, G. Dennler, C. Lungenschmied, and A. J. Mozer, Energy Environ. Sci. **5**, 5241 (2012).
[19] D. Rauh, C. Deibel, and V. Dyakonov, Adv. Funct. Mater. **22**, 3371 (2012).
[20] A. Foertig, J. Kniepert, M. Gluecker, T. Brenner, V. Dyakonov, D. Neher, and C. Deibel, Adv. Funct. Mater. **24**, 1306 (2014).
[21] T. M. Clarke, F. C. Jamieson, and J. R. Durrant, J. Phys. Chem. C **113**, 20934 (2009).
[22] A. Foertig, A. Baumann, D. Rauh, V. Dyakonov, and C. Deibel, Appl. Phys. Lett. **95**, 052104 (2009).
[23] G. Juška, K. Genevičius, N. Nekrašas, G. Sliaužys, and R. Österbacka, Appl. Phys. Lett. **95**, 013303 (2009).
[24] C. G. Shuttle, R. Hamilton, J. Nelson, B. C. O'Regan, and J. R. Durrant, Adv. Funct. Mater. **20**, 698 (2010).
[25] T. Kirchartz and J. Nelson, Phys. Rev. B **86**, 165201 (2012).
[26] C. Deibel, D. Rauh, and A. Foertig, Appl. Phys. Lett. **103**, 043307 (2013).
[27] A. Pivrikas, G. Juška, A. J. Mozer, M. Scharber, K. Arlauskas, N. S. Sariciftci, H. Stubb, and R. Österbacka, Phys. Rev. Lett. **94**, 176806 (2005).
[28] G. Juška, K. Arlauskas, G. Sliaužys, A. Pivrikas, A. J. Mozer, N. S. Sariciftci, M. Scharber, and R. Österbacka, Appl. Phys. Lett. **87**, 222110 (2005).
[29] C. G. Shuttle, B. O'Regan, A. M. Ballantyne, J. Nelson, D. D. C. Bradley, and J. R. Durrant, Phys. Rev. B **78**, 113201 (2008).
[30] L. J. A. Koster, V. D. Mihailetchi, and P. W. M. Blom, Appl. Phys. Lett. **88**, 052104 (2006).
[31] M. C. Scharber, M. Koppe, J. Gao, F. Cordella, M. A. Loi, P. Denk, M. Morana, H.-J. Egelhaaf, K. Forberich, G. Dennler, R. Gaudiana, D. Waller, Z. Zhu, X. Shi, and C. J. Brabec, Adv. Mater. **22**, 367 (2010).
[32] T. M. Clarke, D. B. Rodovsky, A. A. Herzing, J. Peet, G. Dennler, D. DeLongchamp, C. Lungenschmied, and A. J. Mozer, Adv. Energy Mater. **1**, 1062 (2011).
[33] D. H. K. Murthy, A. Melianas, Z. Tang, G. Juška, K. Arlauskas, F. Zhang, L. D. A. Siebbeles, O. Inganäs, and T. J. Savenije, Adv. Funct. Mater. **23**, 4262 (2013).
[34] S. Albrecht, S. Janietz, W. Schindler, J. Frisch, J. Kurpiers, J. Kniepert, S. Inal, P. Pingel, K. Fostiropoulos, N. Koch, and D. Neher, J. Am. Chem. Soc. **134**, 14932 (2012).
[35] G.-J. A. H. Wetzelaer, N. J. van der Kaap, L. J. A. Koster, and P. W. M. Blom, Adv. Energy Mater. **3**, 1130 (2013).
[36] S. Roland, M. Schubert, B. A. Collins, J. Kurpiers, Z. Chen, A. Facchetti, H. Ade, and D. Neher, J. Phys. Chem. Lett. **5**, 2815 (2014).
[37] A. J. Mozer, G. Dennler, N. S. Sariciftci, M. Westerling, A. Pivrikas, R. Österbacka, and G. Juška, Phys. Rev. B **72**, 035217 (2005).
[38] G. Dennler, A. J. Mozer, G. Juška, A. Pivrikas, R. Österbacka, A. Fuchsbauer, and N. S. Sariciftci, Org. Electron. **7**, 229 (2006).
[39] T. M. Clarke, J. Peet, A. Nattestad, N. Drolet, G. Dennler, C. Lungenschmied, M. Leclerc, and A. J. Mozer, Org. Electron. **13**, 2639 (2012).
[40] J. Szmytkowski, Chem. Phys. Lett. **470**, 123 (2009).
[41] C. Deibel, A. Wagenpfahl, and V. Dyakonov, Phys. Rev. B **80**, 075203 (2009).
[42] M. Hilczer and M. Tachiya, J. Phys. Chem. C **114**, 6808 (2010).
[43] I. A. Howard, R. Mauer, M. Meister, and F. Laquai, J. Am. Chem. Soc. **132**, 14866 (2010).
[44] A. J. Ferguson, N. Kopidakis, S. E. Shaheen, and G. Rumbles, J. Phys. Chem. C **115**, 23134 (2011).
[45] R. Hamilton, C. G. Shuttle, B. O'Regan, T. C. Hammant, J. Nelson, and J. R. Durrant, J. Phys. Chem. Lett. **1**, 1432 (2010).
[46] M. C. Heiber, "ISING_OPV," https://github.com/MikeHeiber/Ising_OPV.
[47] M. C. Heiber and A. Dhinojwala, Phys. Rev. Applied **2**, 014008 (2014).
[48] A. Miller and E. Abrahams, Phys. Rev. **120**, 745 (1960).
[49] A. V. Nenashev, F. Jansson, S. D. Baranovskii, R. Österbacka, A. V. Dvurechenskii, and F. Gebhard, Phys. Rev. B **81**, 115204 (2010).
[50] G. A. H. Wetzelaer, M. Kuik, H. T. Nicolai, and P. W. M. Blom, Phys. Rev. B **83**, 165204 (2011).
[51] See Supplemental Material at http://link.aps.org/supplemental/10.1103/PhysRevLett.114.136602 for morphology generation details, a full list of simulation parameters, and supplemental results.